applied optics

Vibratory strain field measurement by transverse digital holography

KARL A. STETSON

Karl Stetson Associates, LLC, 2060 South Street, Coventry, Connecticut 06238, USA (kastetson@holofringe.com)

Received 10 June 2015; revised 24 August 2015; accepted 24 August 2015; posted 31 August 2015 (Doc. ID 242829); published 17 September 2015

A method is presented for measuring vibratory strain fields using phase-stepped, image-plane digital holography. An object surface is observed along its normal vector while illuminated at equal and opposite angles by two mutually coherent laser beams. One beam is phase stepped by quarter-wavelength increments between TV frames, and the resulting images are processed to yield holographic images. Object vibrations result in zero-order Bessel function fringes in the display. The second beam is modulated at the same frequency of the object vibration and is used to shift the fringes in a manner analogous to phase step interferometry. The resulting images are processed to yield a wrapped phase map, which is unwrapped and corrected for the error associated with using zero-order Bessel functions in place of cosine functions. The unwrapped images are processed to obtain the average slopes for image segments, and these slopes are multiplied by a scale factor to convert them to strain. The analysis program used here divides the field of view into five horizontal by four vertical segments, which provide a map of the vibratory strain field.

OCIS codes: (120.2880) Holographic interferometry; (120.3940) Metrology; (120.6160) Speckle interferometry.

http://dx.doi.org/10.1364/AO.54.008207

1. INTRODUCTION

The optical configuration introduced by Leendertz in 1970 [1] has been used to obtain in-plane strains for static deformations; however, to this author's knowledge it has never been used to measure vibratory strain. The initial reason for this was that object displacements were detected as cyclic changes in speckle patterns. The object surface is illuminated by two mutually coherent laser beams at equal and opposite angles to the surface normal, along which it is observed. The surface reflects a field with random phase modulation for each illumination, and the interference in these fields is observed. As the phase between the two beams changes, the observed speckles will change and decorrelate with the original pattern. When the phase change is one complete cycle, however, the observed speckles will form their same initial pattern, and this repetition can be detected by speckle correlation to yield fringes. Speckle correlation, however, does not lend itself to the analysis of vibratory motions.

The use of phase stepping [2,3], however, changed the way object displacements can be measured by this technique. If three or more images are recorded for known phase steps, it is possible to compute the equivalent of a holographic image, even though both fields are randomly speckled. Either field may be considered the "object" field and the other a "reference" field, and the reference field forms a transmission function through which the object is observed. [4] A vibratory motion of the object will generate a fringe pattern proportional to a zero-order Bessel function of the first kind, and this pattern multiplies the irradiance of the object that has been calculated from the phase-stepped images. This happens even though the object field is not combined with a smooth reference field. When a speckled reference field is used, the speckled texture is increased in the object image.

A technique that may be referred to as pseudo-phase-step interferometry has been used for vibration analysis for many years. [5] In this technique, the Bessel function fringes are shifted by introduction of a bias vibration in the reference beam at the same frequency and phase as the object vibration. Bessel function fringes are nearly periodic, and, if they shifted by appropriate amounts, the resulting images can be processed as if they were cosine fringes to yield wrapped phase images. These images can be unwrapped and the results corrected for the error that results from the difference between Bessel and cosine fringes. Thus, in the experiments reported here, one beam is phase stepped to provide images that are processed to form a real-time holographic reconstruction. The other beam is phase modulated at the frequency and phase of the object vibration to shift the zero-order Bessel function fringes.

2. EXPERIMENTS

A. Setup

Figure 1 shows the layout of the components used in these experiments. A helium–neon laser beam was directed through a

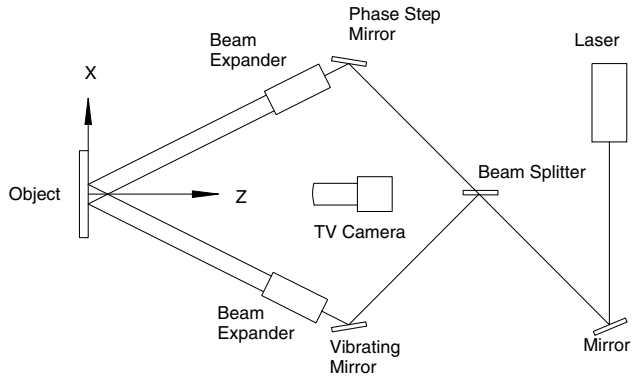

Fig. 1. Component layout for vibratory strain measurement.

beam splitter and reflected from two piezo-electrically activated mirrors. One provided quarter-wavelength phase steps between TV frames, and the other provided vibration at the frequency of the object. Previous work with this process established that divergence of the illumination beams results in apparent strain when the object is translated, especially toward the camera. Both beams were expanded and collimated, therefore, to eliminate this source of apparent strain. The first object was an aluminum bar 127 mm long by 25.5 mm high by 6.6 mm thick. It was observed via a digital TV camera along the surface normal with a telecentric lens system, and the field of view was 11 mm wide by 8.25 mm high. The object was supported on one edge on two thin wires cemented to a support block and located at the nodes of the first vibration mode. It was stimulated into vibration via eddy currents by an electromagnet driver placed close to the back surface at the center of the bar. The object and its driver were placed on a translation stage so that it could be moved laterally relative to the viewing direction.

B. Data Recording and Analysis

Figure 2(a) shows the real-time image obtained with the camera looking 4 mm left of the center of the aluminum bar. (The frequency of excitation is inset into the upper left of Fig. 2(a) and Fig. 5(a), and this does not enter into the subsequent data processing.) The bright fringe on the right corresponds to the zero argument of the Jo function, and the two dark fringes to the left to its first and second zero values. At the center of the bar, there is no transverse motion, only motion toward and away from the observation direction. To either side of center, there is equal and opposite motion due to the bending of the bar, and this increases with distance from the center. Figure 2(b) shows the wrapped phase obtained from the fringes in Fig. 2(a), shifted by applying a bias vibration to the left illumination beam at the same frequency and phase as the vibration of the bar, and Fig. 2(c) shows the unwrapped and corrected phase.

The details of this procedure have been published [6], so only a brief discussion will be included here. The frequency generator used in this system provides two signals at the same frequency with adjustable relative phase. One is used to vibrate the object and the other to provide a bias phase vibration. The bias vibration is turned on to maximum and set for −170 deg.

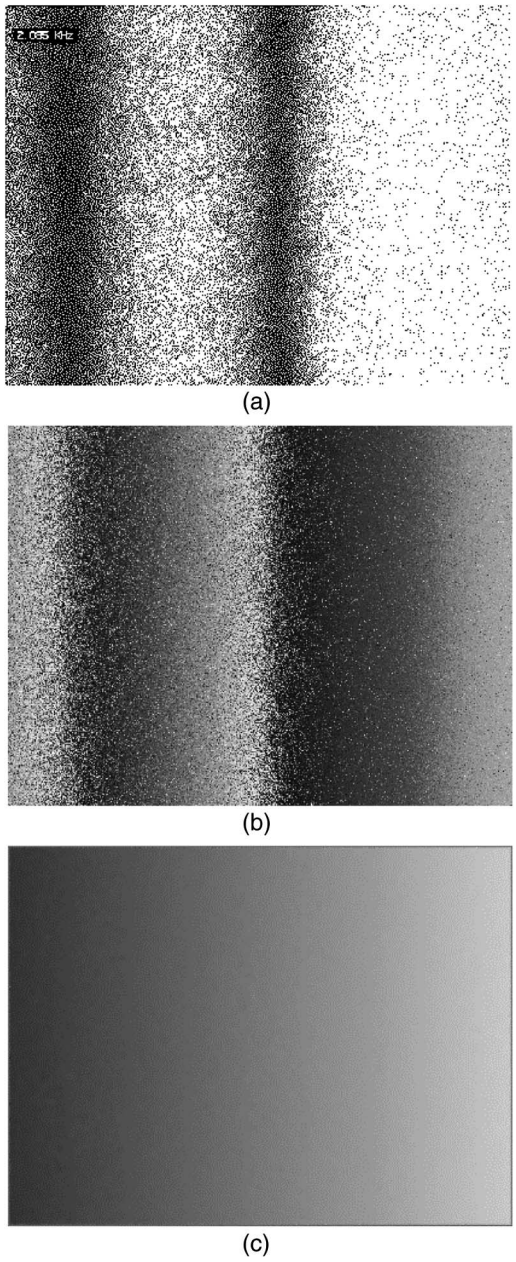

Fig. 2. (a) Real-time image seen of the bar vibrating at 2084.9 Hz, 4 mm left of center. (b) Wrapped phase derived from pseudo-phase shifting of the Jo fringes in 2(a). (c) Unwrapped phase from 2(b), corrected for using Jo fringes as cosine fringes.

The argument of the Jo Bessel function becomes the phasor sum of the object vibration and the bias vibration, and, unless both are at the same phase, adding the bias vibration generally results in the complete disappearance of the bright zero-order fringe. The bias vibration is incremented phase by +10 deg steps to bring the display to the point where the zero-order fringe will begin to reappear. The zero-order fringe will appear the same over a fairly wide range of bias vibration phase settings, so the operator switches the phase increments to 1 deg and seeks a display that is sharply identifiable such as the zero-order fringe being the same brightness as it neighbor. This

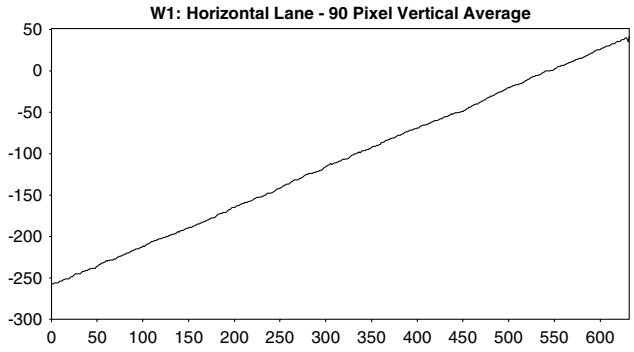

Fig. 3. Horizontal lane of the average of 90 vertical values across the center of Fig. 2(c).

phase value is recorded by the program, the increments increased to 10 deg, and the phase increased through the point where the zero-order fringe reappears to the point where this display duplicates the previously noted image. The phase increment is reduced again to 1 deg for fine adjustment. This phase value is recorded by the program and the average of the two recorded values used for a phase setting. The amplitude of the bias vibration is calibrated by turning the object vibration off and having the operator increase the bias phase vibration until the entire image is black, and the program records that level. The vibration is turned back on, a holographic image recorded, and the program asks the operator to mark a point on the object where the zero-order fringe is located. The program then records holographic images at four values of bias vibration corresponding to $\pm\pi/8$ and $\pm 3\pi/8$ radians. From these, it computes the wrapped phase shown in Fig. 2(b). This data is entered into a phase unwrapping subroutine, and the results have to be read through a lookup table to correct for the errors obtained by using Bessel function fringes as if they were cosine fringes. To do this, the data have to be shifted so that the zero values correspond to the location of the zero-order fringe in the image when no bias vibration is applied. The values are shifted by increments of π radians, therefore, so that the value at the recorded location for the zero-order fringe is as close to zero as possible. The program then applies the proper correction via a lookup table to compensate for the Jo to cosine errors, and the result is the unwrapped image shown in Fig. 2(c).

The unwrapped phase data is scaled so that one cycle of 2π radians of phase corresponds to 256. Figure 3 shows a plot of a lane of values read from the center of the data in Fig. 2(c), in which each point is the average of 90 values in a vertical column. It can be seen that this plot is essentially a straight line with slight deviations.

Strain in the x direction is proportional to the slope of the phase values in the x direction, i.e., the slope of the line plotted in Fig. 3. Rotation and shear are proportional to the slope of the phase values in the y direction. The phase maps are 640 pixels wide by 480 pixels high. A program was written to read the data from 20 sections of an unwrapped phase map, each 127 pixels wide by 119 pixels high, and fit the data for each section to a linear surface in the horizontal and vertical directions for the least-squares error. This gives the average slope of the data in the two directions, x and y. When these values are multiplied by the proper scaling factor, the result is 20 measurements of strain, ε_x, in the field of view. The scale factor is defined [7] by the equation,

$$\varepsilon_x = S_x\lambda/(512 d_p \sin\theta), \tag{1}$$

where S_x is the slope defined as change in pixel value per pixel spacing in the x direction, λ is the wavelength of light (633 nm), d_p is the object distance per pixel in the image (11/640 mm), and θ is the angle between one illumination and the observation direction (27°). Rotation and shear are obtained from the slope in the y direction, as shown in Eq. (2):

$$\gamma - \Phi_x = S_y\lambda/(512 d_p \sin\theta), \tag{2}$$

where γ is the shear, Φ_z is the surface rotation, and S_y is the slope in the y direction. Table 1 shows the values for this data recording.

C. Strain Field Measurement

The strain field in the center of a bar is essentially uniform. In order to get a spatially varying strain field, the bar used in Section 2.B was replaced with the two-sided tuning fork, as shown in Fig. 4.

The camera was aligned to observe the top of the center of the structure, and Fig. 5(a) shows the Jo fringe pattern when it was stimulated into vibration at 969.7 Hz. The wrapped and unwrapped fringes are shown in Figs. 5(b) and 5(c).

The rectangular area in Fig. 5(c) from the top of the structure to just above the holes was divided into 20 segments, 127 pixels wide by 95 pixels high. The data in these segments was fitted to a linear surface for least-squares error, and the slope in

Table 1. Vibratory Strain Near the Center of a Vibrating Bar

(a) Strain values calculated from the x slopes of 20 sectors in the data image of Fig. 2(c). Average of the 20 values is 80.3E – 6.				
78.7E – 6	80.5E – 6	81.4E – 6	79.7E – 6	79.7E – 6
78.3E – 6	79.6E – 6	81.3E – 6	80.4E – 6	80.1E – 6
78.4E – 6	80.5E – 6	81.3E – 6	79.6E – 6	80.5E – 6
77.2E – 6	80.0E – 6	81.3E – 6	79.3E – 6	78.8E – 6
(b) Shear and rotation calculated from the y slopes. The values are essentially zero.				
274.4E – 9	2.1E – 6	1.2E – 6	1.5E – 6	650.8E – 9
725.9E – 9	–402.9E – 9	–1.4E – 6	–830.6E – 9	–565.3E – 9
208.6E – 9	–210.6E – 9	630.5E – 9	404.5E – 9	519.7E – 9
1.6E – 6	590.1E – 9	1.1E – 6	–385.0E – 9	458.4E – 9

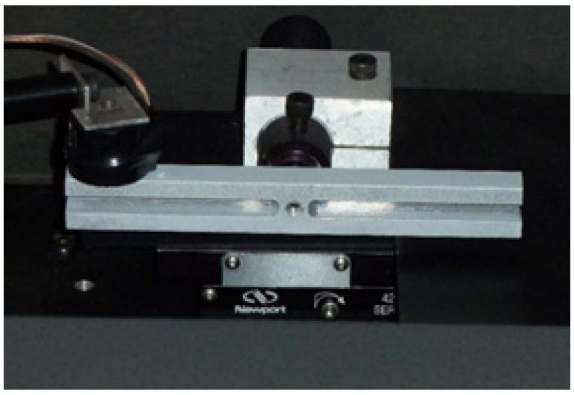

Fig. 4. Two-sided tuning fork used to obtain vibration strain field variations.

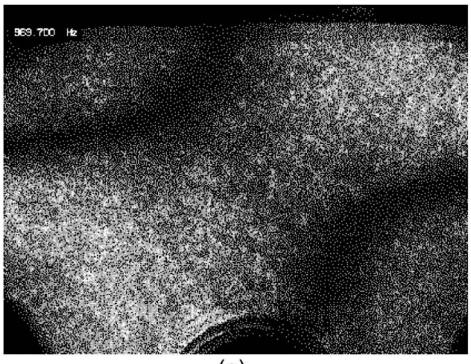

(a)

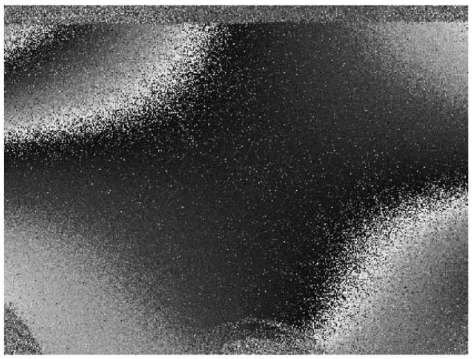

(b)

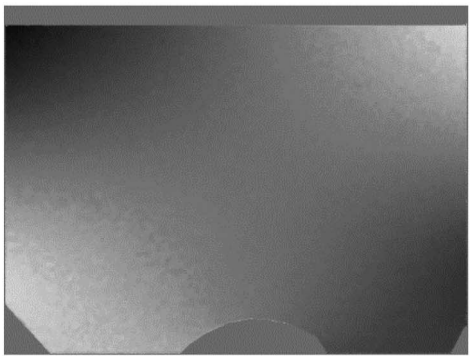

(c)

Fig. 5. Vibratory strain measurement in the upper center of the double tuning fork shown in Fig. 4. (a) Jo fringes for vibration at 969.7 Hz. (b) Wrapped fringes for 5(a). (c) Unwrapped and corrected phase function for the fringes of 5(b).

Table 2. Strain in the *x* Direction (*x* Derivative), and Shear and Rotation (*y* Derivative) for a Double Tuning Fork

(a) Strain distribution in *x* for the data shown in Fig. 5(c)				
−78.7E − 6	−69.6E − 6	−60.3E − 6	−70.4E − 6	−77.2E − 6
−28.1E − 6	−23.0E − 6	−21.7E − 6	−19.3E − 6	−27.3E − 6
26.7E − 6	24.6E − 6	14.4E − 6	22.5E − 6	28.8E − 6
66.0E − 6	66.3E − 6	40.3E − 6	55.1E − 6	65.8E − 6
(b) Shear and rotation for the data shown in Fig. 5(c)				
510.6E − 6	372.4E − 6	253.7E − 6	144.1E − 6	3.2E − 6
262.5E − 6	244.0E − 6	226.2E − 6	208.3E − 6	198.9E − 6
31.7E − 6	132.3E − 6	201.6E − 6	265.7E − 6	358.3E − 6
−135.4E − 6	27.1E − 6	181.7E − 6	306.8E − 6	463.8E − 6

the horizontal direction scaled to give the strain via Eq. (1). The results are shown in Table 2. It can be seen in Table 2(a) that the strain reverses sign going from the top to the bottom of the field of view as would be expected for bending of the upper element. The horizontal variation shows a minimum value in the center.

The shear and rotation shown in Table 2(b) is mostly positive. This data is difficult to interpret because the results are a mixture of two effects. Simultaneous recording with illuminations in the vertical direction [3] would allow complete definition of the strain and rotations.

3. CONCLUSION AND DISCUSSION

It has been shown that vibratory strains can be measured by transverse digital holography. The first example (Section 2.B) shows data recorded near the center of a bar suspended on the nodal points of its first vibration mode. For the excitation used, the strain values measured are 80E − 6 plus or minus a few parts per million. This configuration was chosen in order to obtain sufficient vibration amplitude to generate observable fringes and strain values. Clearly, the field of view can be increased to obtain strain measurements over a larger area in one picture. If a small field of view is used, in the interest of obtaining detailed variations is strain, and it is desired to scan this field of view to cover a larger area, then it will be necessary to provide an accurate vibration sensor to keep the object vibration amplitude the same for each measurement. The second example shown shows variations in strain in the center of the side of a double-sided tuning fork.

One issue that must be considered is that the zero-order fringe of the Jo function may not be observable in the image. This happens in the setup in Section 2.B when the view is moved away from the center of the bar. The phase unwrapping scheme used here has a provision that allows the user to specify that the point marked for the zero-order fringe is actually offset from the zero by a number of π radians, which allows the correction via the lookup table to be applied properly. It may not be known, *a priori*, how many radians are required, but the correct value can be obtained by trial and error because it is obvious when the Jo to cos correction is incorrectly applied. Incorrect compensation results in a noticeable ripple in the unwrapped phase function.

REFERENCES

1. J. A. Leendertz, "Interferometric displacement measurement on scattering surfaces utilizing speckle effect," J. Phys. E **3**, 214–218 (1970).
2. P. K. Rastogi, "Measurement of static surface displacements, derivatives of displacements, and three-dimensional surface shapes—examples of applications to non-destructive testing," in *Digital Speckle Pattern Interferometry and Related Techniques* (Wiley, 2001), pp. 141–224.
3. A. J. Moore and J. R. Tyrer, "Two-dimensional strain measurement with ESPI," Opt. Lasers Eng. **24**, 381–402 (1996).
4. K. A. Stetson, "Phase-step digital holography with speckled reference beams," Appl. Opt. **54**, 4116–4119 (2015).
5. K. A. Stetson and W. R. Brohinsky, "A fringe shifting technique for numerical analysis of time-average holograms of vibrating objects," J. Opt. Soc. Am. A **5**, 1472–1476 (1988).
6. K. A. Stetson, "Effect of phase mismatch on pseudo-phase-step analysis of time-average hologram recordings of vibration modes," Appl. Opt. **45**, 6473–6476 (2006).
7. K. A. Stetson, "Strain field measurement by transverse digital holography," Appl. Opt. **54**, 6065–6070 (2015).